

Anomaly of surface circulation and Ekman transport in Banda Sea during 'Normal' and ENSO episode (2008-2011)

Selfrida M. Horhoruw¹, Agus S. Atmadipoera^{1*}, Pieldrie Nanlohy² and I Wayan Nurjaya¹

¹Department of Marine Science and Technology, FPIK IPB Bogor

²Department of Physics, FMIPA UNPATTI Ambon

E-mail: atmadipoera_itk@ipb.ac.id, idahorhoruw@gmail.com

Abstract. Banda Sea (BS) is a deep and large ocean basin in interior Indonesia Seas which may play a significant role on regulating ocean dynamics and regional climate variability such as El Nino Southern Oscillation (ENSO). It also provides a 'temporary reservoir' for Indonesian Throughflow (ITF), and as a region of seasonal alternating upwelling/downwelling. The objective of present study is to investigate changes of surface ocean circulation and associated upwelling anomaly during 'normal' (2008/2009), El Nino (2009/2010) and La Nina (2010/2011) years in BS, using data sets from validated INDESO model outputs. The results show that surface circulation in BS is regulated by both local forcing of monsoon winds and inflow of ITF via Flores Sea (FS), Lifamatola Strait, and Halmahera/Seram Seas. Inflow from FS is drastically increased during northern winter and 'normal' year. The upwelling event occurs along the eastern edge of BS with southwestward Ekman transport and its kinetic energy of above 10 Joule. The Ekman layer depth in BS is about 60 m. During La Nina event surface circulation is much stronger with kinetic energy of about 700 J, causing Ekman layer shallower due to increased Ekman transport and upwelling intensity.

1. Introduction

Banda Sea (BS) is one of important fishing ground areas for pelagic fisheries in Indonesia, due to the upwelling processes that impact positively on high primary productivity [1]. Furthermore, BS is a unique confluence region of different water masses, originated from North and South Pacific Ocean [e.g., 3, 9].

The seasonal reversal monsoonal winds are fully developed here during peaks of the Northwest monsoon (December-February) and Southeast monsoon (July-September) periods, causing seasonal reversal of upper ocean circulation, known as the Indonesian monsoon current (or Armondo). During the Northwest monsoon (NWM) period, Armondo transports water masses from the Java and Flores Seas into BS, resulting in accumulation of water masses and causing downwelling. During the Southeast monsoon (SEM) period, Armondo brings water masses westward from Banda, so there is an imbalance of water mass volume which generate a vertical movement of water masses from deeper to surface layers (or upwelling) [1, 2]. Circulation in BS is also affected by interannual climatic variability such as El Nino Southern Oscillation (ENSO). It is found that during the El Nino phase, seawater temperature is much cooler related to weakening Ekman pumping than that during the La Nina event [3].



Theoretically, upwelling event is associated with Ekman pumping and Ekman transport of water mass. Those are generated by the steady and strong winds fields. Ekman transport plays an important role on transporting water masses away from the center of upwelling region. Due to the Earth rotation, wind-driven surface currents are deflected about 45° to the right (left) to the winds direction in the northern (southern) hemispheres [4]. In BS, peak of Ekman upwelling occurs in May and June with upwelling transport volume of 2.5 Sv ($1 \text{ Sv} = 10^6 \text{ m}^3 \text{ s}^{-1}$), but peak of Ekman downwelling occurs in February with transport volume of 1.0 Sv [3].

This paper aims to investigate changes of surface circulation patterns during 'normal' 2008/2009, El Nino 2009/2010 and La Nina 2010/2011 events (hereinafter referred to as 'normal', El Nino and La Nina), and its implication to Ekman layer and upwelling intensity in BS. Since anomaly of interannual climatic variability such as ENSO impacts significantly on ocean-atmosphere interaction and marine ecosystem in Indonesian Seas, particularly in Banda Sea, so this study may provide the first insights into a better understanding of circulation anomaly in BS during ENSO year 2009/2011.

2. Data and data analysis

2.1. Study area

This study was conducted from May to August 2016 in the Physical Oceanography Laboratory, Department of Marine Science and Technology (ITK) - FPIK IPB Bogor. The study area is in deep BS basin (figure 1). Lines that parallel and perpendicular to the eastern outer islands arcs of BS denote sections for Ekman transport and upwelling calculations.

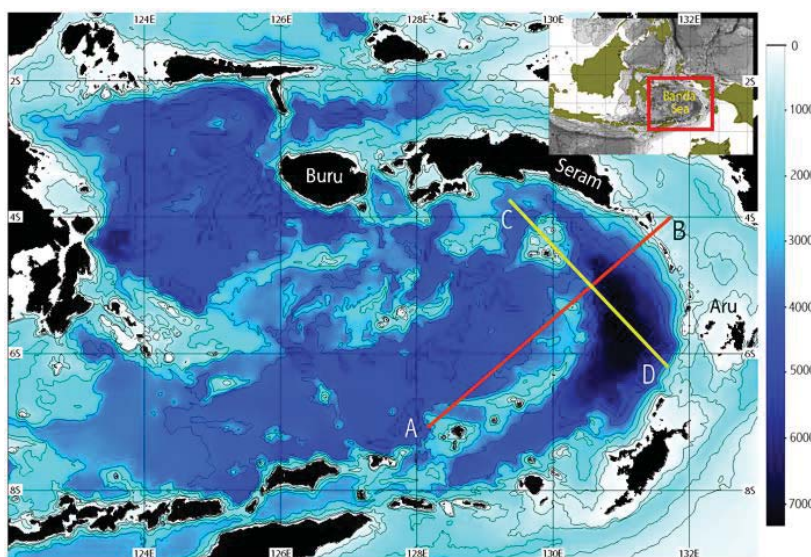


Figure 1. Bathymetry in study area in BS. Lines of A-B and C-D denote for cross-coast velocity and along-coast velocity for further calculations of Ekman upwelling with a reference to BS outer-islands arcs between Seram and Aru Islands. Interval of contour is every 1000 m.

2.2. The data

2.2.1. INDES0 model outputs

Model outputs from a series of simulation of NEMO ocean general circulation model of INDES0 configuration (INDES0: Infrastructure Development of Space Oceanography), performed by the CLS France & BPOL Bali, were used in this study. The outputs of data-series span from June 1st 2008 to May 31 2011, covering 'normal' and ENSO years. INDES0 is a scientific cooperation program at the Ministry of Marine Affairs and Fisheries with a consortium of joint European Marine Research Institute

(MERCATOR-Ocean and *Collecte Localisation Satellites* - CLS) France. A brief description of INDES0 configuration is illustrated here. The model used 3-dimensions NEMO modeling system, developed by [5]; Atmospheric forcing is derived from the ECMWF reanalysis data with temporal resolution of 6-hours; Both barotropic and baroclinic tidal forcing was applied explicitly to the model; Lateral boundary forcing was extracted into the model from the $1/4^\circ$ global ocean circulation of Mercator-Ocean; Horizontal grid resolution is $1/12^\circ$ (approximately 9.25 km) with 50 depth levels; bathymetry of the model is derived from ETOPO02 data [6]. Model simulation was covered from 2008 to 2015. Daily averaged of 3-dimensions seawater temperature, salinity and ocean current fields were used for this study.

2.3. Model validation

To assess a performance and reliability of the model results, time-series data of sea surface temperature anomaly (SSTA) and sea surface height anomaly (SSHA) from the model outputs were compared with those observed from the NOAA AVHRR high-resolution SST data and AVISO satellite altimetry data, in the center basin of BS (figure 2; inset). A statistical correlation coefficient between SSTA and SSHA model output and the data are reasonably high of 0.99 and 0.94, for SSTA and SSHA, respectively. It is shown clearly that fluctuations of SSTA and SSHA both in the model and data are in excellent agreement. The SSTA time-series data reveal strong seasonal variations, which are minima during the SEM period and double maxima during the monsoon transition and peak of the NWM periods (figure 2A). Furthermore, SSHA minima occur during the peak of SEM period and their maxima are during the peak of NWM (figure 2B). These results are consistent with [3]. Hence, model outputs of SST and SSH from INDES0 model reproduced well the observed satellite data and can be used for further analysis in this study.

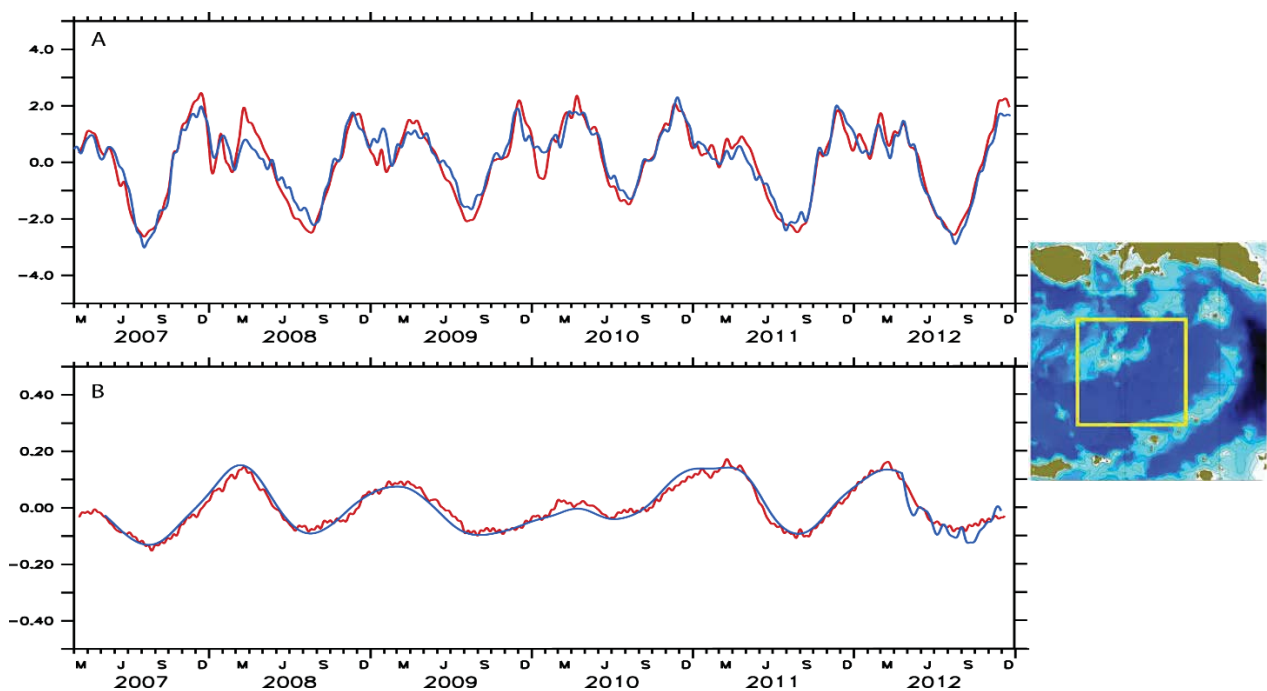


Figure 2. Time-series of sea surface temperature anomaly (A) and sea surface height anomaly (B) from the INDES0 model output (red) and satellite data (blue). The data were extracted from a sampling box at the center of BS (see inset map). Statistical correlation coefficient for SSTA and SSHA are 0.94 and 0.96, respectively. Plot of time-series data are smoothed by 21-day Hanning low-pass filtered.

2.3. Data analysis

The 3-dimensions time-series data of INDESO model of seawater temperature, salinity and zonal & meridional current components, and time-series data of El Nino Southern Oscillation (ENSO) indices (NINO3.4 and SOI) between 2008 and 2011 were analyzed to understand monthly evolution of oceanic conditions (circulation and seawater properties distribution) during 'normal' year, El Nino and La Nina years.

Surface kinetic energy (KE) was calculated from ocean current fields and was analyzed to understand circulation pattern and upwelling dynamic in BS, using the equation as follows:

$$KE = \frac{1}{2} \rho V^2 \quad (1)$$

where V is total current vector of zonal and meridional components, and ρ is seawater density.

To obtain cross-coast velocity that will be calculated for Ekman transport and vertical cross-section of upwelling evolution, zonal (u) and meridional (v) current components were rotated anticlockwise by 45° from a reference of the BS islands arc between Seram and Aru Islands with the northwest-southeast orientation (see figure 1). According to [7], rotated current component (u and v) from the North reference into local reference with θ is presented in equation 2 and 3, as follows [7]:

$$U' = u \cos \theta + v \sin \theta \quad (2)$$

$$V' = -u \sin \theta + v \cos \theta \quad (3)$$

where, u and v are zonal and meridional current components; θ is degree of rotation with local reference; U' and V' are rotated cross-coast velocity (CCV) and along-coast velocity (ACV). Illustrations of CCV and ACV are shown in Fig. 1, as A-B line and C-D line, respectively.

Analysis of monthly averaged current fluctuation was focused in the CCV transect (A-B line, in Fig. 1). Furthermore, Ekman transport was calculated across the ACV transect (C-D line, in Fig. 1). Based on this calculation, magnitude and direction of Ekman transport volume away from the reference (islands) is considered to be upwelling parameter. Ekman transport volume estimate (Q) was calculated across C-D section (Fig.1) using the equation below:

$$Q = \sum_{k=1}^n V' A \quad (4)$$

where V' is the cross-coast velocity (CCV) perpendicular to the BS islands arc that obtained from equation (3), and A is cross-sectional area for i^{th} grid, and $k=1$ to n is number of grids.

3. Results and discussion

3.1. Surface circulation during 'normal', El Nino, and La Nina years

Monthly mean of kinetic energy and current vectors during the SEM and NWM periods in three different years are presented in figure 3. Evolution of monthly surface circulation during 'normal' and ENSO events (2008-2011) showed that the surface flow in BS is driven by monsoonal winds and is also influenced by upper component of Indonesian Throughflow (ITF) that is derived from three main inflows via Flores Sea, Lifamatola Strait and Halmahera Sea. Previous studies showed that the main transport volume of ITF pass by the western route via Sulawesi Sea-Makassar Strait-Flores Sea [8-11]. Large seasonal reversal flows are related to seasonal changes of monsoonal winds over the study area [3, 12].

In general, the KE and current vectors showed high amplitude of surface currents in Flores Sea during the NWM period, which is coherent with strong surface winds over BS. High kinetic energy in the entrance of Flores Sea apparently brings surface water mass derived from western part of interior seas, such as Makassar Strait, Java Sea and southern South China Sea [2, 13, 26]. From December to January, surface current in eastern Flores Sea turned to the North along the western edge of Buru Island and joined surface current from Lifamatola Strait. So that, circulation in Seram Sea is indicated by eastward flows that may be a confluence region of different water masses from Flores Sea and Maluku Sea/Lifamatola Strait. This

is consistent with [2], during the NWM period, surface water flows eastward and enters Halmahera and Maluku Seas. From February to March, counter-clockwise circulation (eddy) was found in northwestern BS.

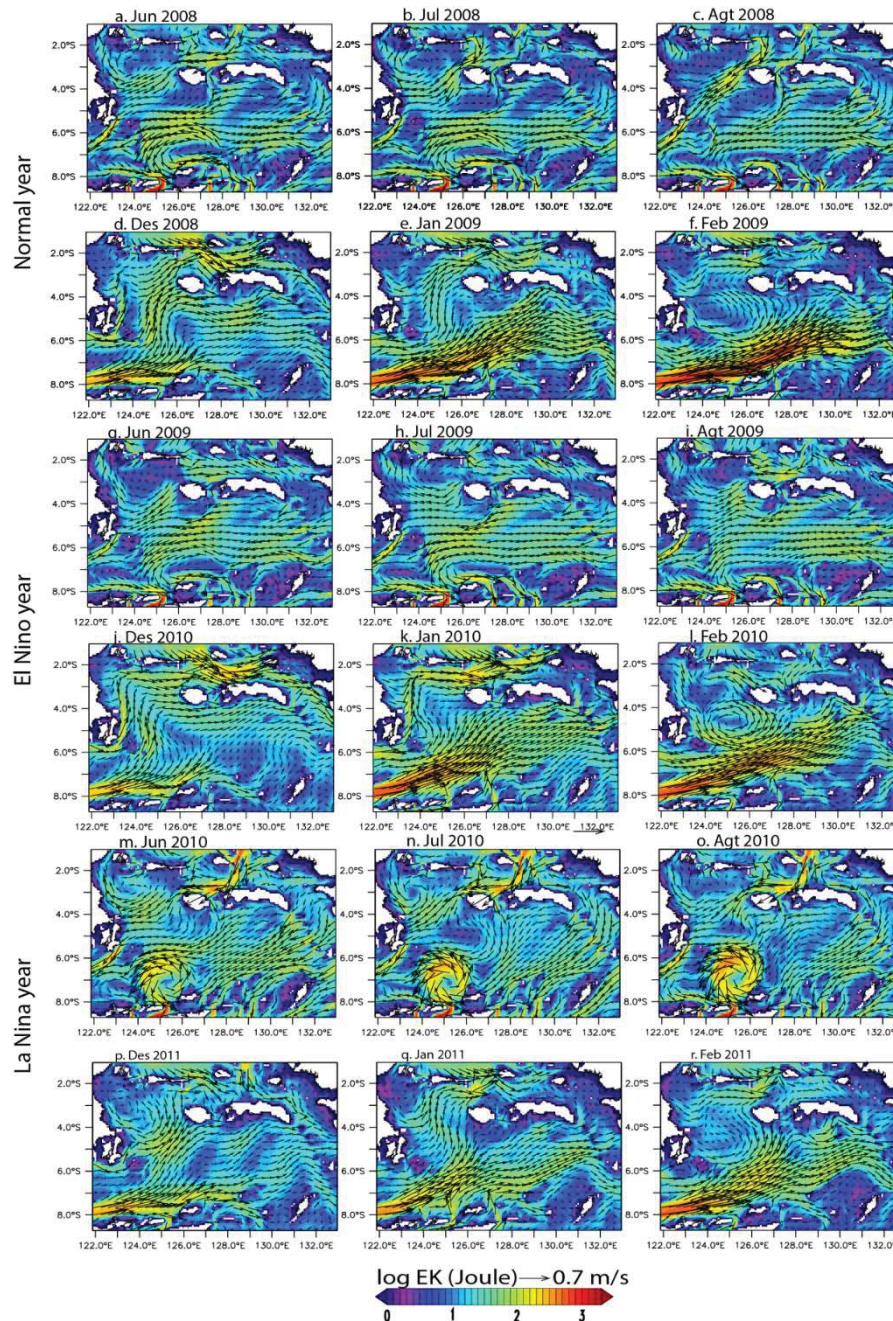


Figure 3. Monthly surface kinetic energy, overlaid with current vectors during the Southeast monsoon (SEM) and Northwest monsoon (NWM) periods in 'normal', El Nino and La Nina in BS.

The fully developed SEM winds cause reversal of surface circulation patterns, where surface current in Halmahera Sea becomes much stronger. Surface current in Halmahera flows westward along the northern edge of Seram Island and small branch of these currents enter Buru Strait where the other current down the western edge of Buru Island. During this period, a high kinetic energy anti-clockwise eddy was formed in

the Southwest Maluku Island. The existence of this eddy was relatively permanent during the SEM period. Its size and kinetic energy varied during different ENSO period. Radius of eddy formation was about 300 km. According to [2, 13], the wind-driven currents in BS pushes back surface water from eastern BS westward into Flores Sea, thus weakening the flow in Flores Sea. Formation of anti-clockwise eddies in southern hemisphere causes a convergent circulation that leads to water mass sinking (downwelling), while clockwise eddies, enhanced by the SEM winds, cause a divergent circulation in eastern Banda region, transporting surface water mass away from the coastal area between Seram and Aru Islands. This offshore transport is compensated by upwelled water from deeper layer to surface layer to maintain continuity of seawater volume. [3] revealed that surface divergent circulation influences significantly on surface component of ITF in BS.

Variation of surface circulation in BS is also affected by the ENSO phenomena. During the SEM period in 'normal' year 2008 (figure 3), the flow via Halmahera Sea branched, where one part flows down along northern Obi Island and the rest turns into Seram Sea through Lifamatola Strait. Surface circulation is predominantly westward to western Seram Sea and merges with the flow from Lifamatola Strait. In addition, there a northward flow along the eastern boundary of Papua Island near 1°S latitude.

Hence, during 'normal' year 2008 the main inflow for circulation in BS was via Halmahera Sea and Lifamatola Strait through Buru Strait (western part of Seram Island) and western part of Buru Island. Furthermore, a divergent circulation occurs between eastern part of Seram and western side of Papua (near ~1°S), where the northward flow was predominant. During this period, upwelling also occurs in western part of Papua. Previous studies reported the occurrence of less salty water from eastern Papua [2, 14, 15]. The westward flow into BS from eastern side brings surface water away from eastern Banda Islands arcs, which extends from southern Buru Island to northern Southwest Maluku. This implies a generation of upwelling event during the SEM period.

During the SEM period in the El Nino event 2009, the main inflow from Halmahera and Lifamatola that supply surface flow in BS was reduced, but the divergent circulation in western Papua (~ 1°S) strengthened, where one branch of the current flows northward up to northern Buru which push back surface water into Halmahera Sea and Lifamatola Strait, and part of current branch enters BS via its eastern side (figure 3).

During the SEM period in La Nina event 2010, the trade winds in the equatorial Pacific were much stronger [16, 17], which increased an accumulation of 'warm pool' in western equatorial Pacific. Furthermore, a 'leakage' of ITF inflow via Halmahera Sea and the Lifamatola Strait also strengthened during this period, and divergent circulation in western Papua decreased (figure 3 m-o). Sea surface height anomaly in BS during La Nina event was much higher, compared to 'normal' and El Nino years (figure 2b) [3]. During this event, eddies formation in northern Southwest BS was developed much stronger with kinetic energy of about 400 Joule, and eddies diameter of about 290 km (Fig. 3o). During late of the SEM and transition monsoon periods the divergent circulation in BS was weakened (not shown).

During the NWM period in 'normal' year 2008, surface circulation in Flores Sea was much stronger with the highest kinetic energy was found in its main axis of about 100-750 Joules (figure 3 d-f). The maximum kinetic energy was also found in northern Alor (7-9°S and 123°E). However, during the NWM period in El Nino year 2009, surface circulation in Flores Sea was reasonably reduced in February with averaged kinetic energy in its main axis between 100-680 Joule.

Surface flows in eastern Flores Sea weakened during the NWM period in La Nina event 2010 with kinetic energy between 50-600 Joules, but kinetic energy of the circulation increased above 700 Joule in March (not shown). Inflow into BS was also increased (figure 3 p-r). This suggests that there was about a month phase delay of circulation peak during La Nina, compared to El Nino and 'normal' years. It is considered that much stronger kinetic energy of surface circulation via Flores Sea during La Nina event was associated with an increased flow of ITF along its western pathway [11, 18-20].

3.2 Surface temperature and salinity anomaly during 'normal' and ENSO years.

It is interesting to note that during the SEM 'normal' year 2008, SST anomalies in BS were much lower (negative) (figure 4a). However, in the El-Nino event 2009/2010, positive SST anomalies were seen in western BS, while negative anomalies occurred in eastern and northern region (figure 4b). During La Nina year 2010/2011 much higher positive anomalies of SST were evident in BS with weak negative anomalies occurred in eastern Flores Sea (figure 4c).

It is expected that SST variation during El Nino event is much lower than that during 'normal' year [3]. It is suggested that during El Nino year SST anomaly is much cooler related to weakening Ekman pumping, in contrast to those observed during La Nina year [3]. In contrary, here, during 'normal' year 2008 mean SST distribution varied between 26.7 and 29.1°C, which was much cooler than that during El Nino year (28.8 and 29.5°C). This is consistent with observed time-series SSTA data in Fig. 2, showing that SSTA minima during 2008 ('normal' year) was much lower than that during 2009 (El Nino year). It is likely that weak El Nino 2009/2010 may be a possible explanation to this anomalous warmer SST during El Nino year. But, further study is needed to understand its mechanism. During strong La Nina 2010/2011 SST in BS was much warmer than 'normal' year, which is in good agreement with [21].

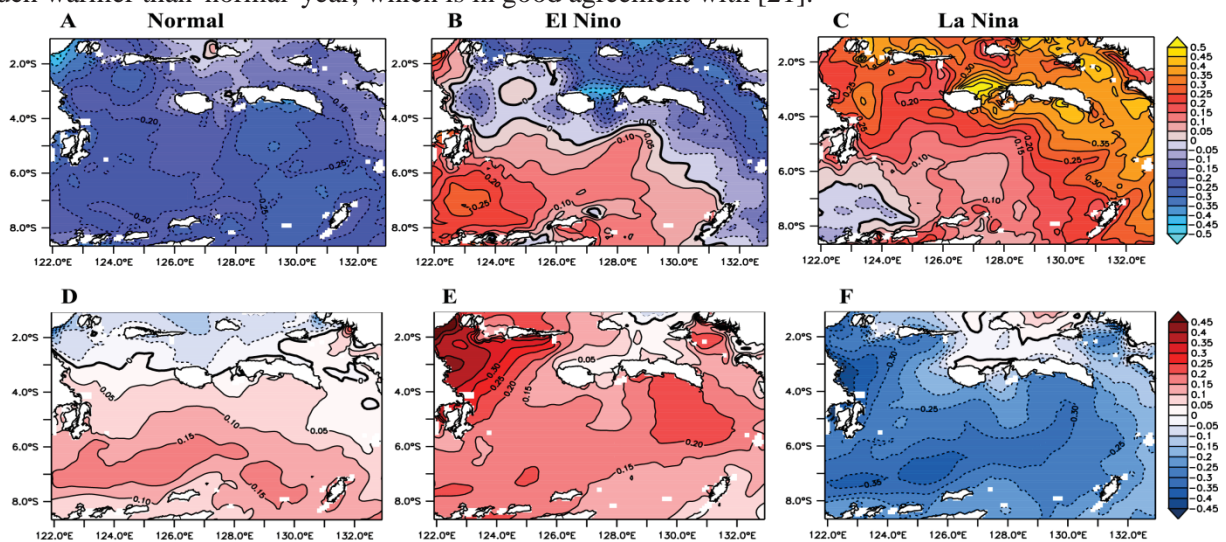


Figure 4. Anomaly of sea surface temperature (A-C) and salinity (D-F) in BS during 'normal' year 2008 (A and D), El Nino year 2009/2010 (B and E), and La Nina year 2010/2011 (C and F).

Furthermore, cross-section of seawater temperature along the C-D transect (not shown) showed that during the SEM in 'normal' year 2008, SST minima varied between 26.0 and 27.5°C with the Ekman depth of about 70 m in August 2008. During El Nino 2009/2010 surface temperature was about 0.5°C higher than that during 'normal' year 2008 of about 27-28.5°C and Ekman layer is shallower to about 60 m. During the SEM in La Nina year 2010/2011, surface temperature varied from 27 to 28.5°C and Ekman layer was much shallower (about 40 m).

Strong positive salinity anomalies were identified during El Nino year (figure 4e), while low salinity anomalies were found during La Nina year (figure 4f). Positive salinity anomalies were increased by about 0.15 psu during El Nino year, compared to salinity in 'normal' year and also higher than La Nina year with different salinity anomalies about 0.4 psu. Cooler surface temperature and saltier water masses in BS during El Nino create much denser water that decrease sea surface height [3,21]. Much denser surface water masses are associated with shallower mixed layer. Much saltier salinity during El Nino (Fig. 4e) may be associated

with a loss of direct precipitation, since convective clouds shifted eastward from western equatorial Pacific. In contrast, during La Nina year (figure 4f), high precipitation rate was impact directly to a decrease of surface salinity.

High surface temperature variation was found in eastern BS (not shown), associated with upwelling events during the SEM period, and weak surface temperature variation occurs during La Nina 2010. However, surface salinity variation was high in northeastern BS and in eastern Flores Sea. Surface monsoon current flows eastward during the NWM period caused high surface salinity variation in western boundary of BS [15, 23].

3.3 Variation of Ekman transport during 'normal', El Nino and La Nina years

During the SEM period both in 'normal' and ENSO years, Ekman transport in the Ekman layer (55.76 m) was negative which means that transport direction was away from the coastal region in the eastern BS between Seram and Aru Islands. This is indicated by negative values and blue color (figure 5a). Consequently, upwelled water mass from deeper layer into the sea surface layer must be taken place to compensate transported water volume offshore. In contrary, during the NWM period in 'normal' and ENSO period, the Ekman transport direction was toward the coastal region (positive values; red color), where accumulation of surface warm and less salty water develop downwelling process. Those dynamics of divergence and convergence appear seasonally as a response of surface layer in BS to the monsoonal winds [3, 14, 22].

In 'normal' year 2008, the southwestward (negative) Ekman transport maximum was about 1.84 Sv ($1\text{Sv} = 10^6 \text{ m}^3\text{s}^{-1}$). During the SEM period in El Nino year the Ekman transport was slightly decreased by 1.58 Sv with one-month lead in June, while in La Nina year the offshore Ekman transport maximum was about 1.24 Sv in June (figure 5b).

In contrary, the convergent (positive) Ekman transport towards the coastal waters occur during the peak of NWM period. In 'normal' year 2008, the peak of positive Ekman transport revealed two maxima in December 2008 and February 2009 with averaged transport of 1.4 and 1.61 Sv. During El Nino year 2009/2010, the divergent (positive) transport maximum was 2.6 Sv. However, in La Nina year 2010/2011 the divergent transport toward the coastal region was decreased to 2.12 Sv. Interestingly, the divergent (positive) transport maximum occurred during El Nino year 2009/2010 which was relatively short duration, from December 2009 to April 2010. However, during La Nina year 2010/2011 the divergent transport was much longer in duration from September 2010 to April 2011 (figure 5).

4. Conclusion

Surface circulation in BS is mainly driven by local reversal monsoonal winds, and influenced by upper component of the ITF. Its magnitude and spatial variation of surface circulation are significantly modified during the ENSO year. Model suggested that during the SEM period in El Nino year 2009/2010 surface inflow from Lifamatola and Halmahera was weakened and in western Papua waters a divergent circulation was established. In La Nina year 2010/2011 the inflow from northern Banda was increased drastically, which diminished divergent circulation in western Papua and increased sea surface height in BS. Transient eddies with high kinetic energy were formed in southwest BS only during La Nina event. During the NWM period, the inflow from Flores Sea into BS was increased.

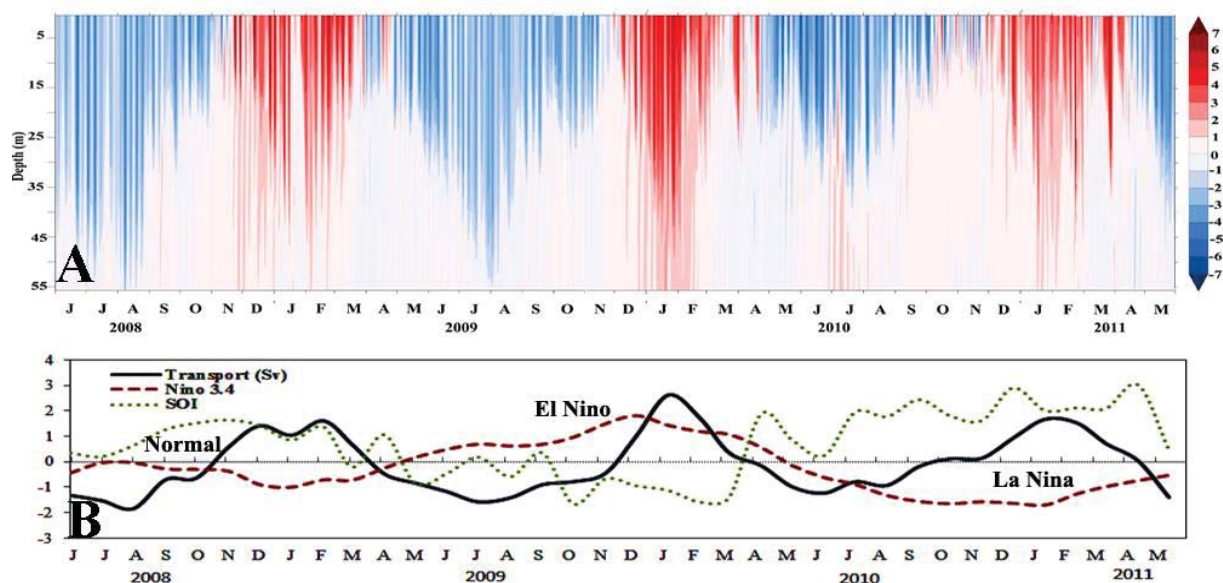


Figure 5. (A) The average of Ekman transport between surface and 56 m depth along the C-D transect (see figure 1); and (B) time-series data of total Ekman transport, Nino3.4 and SOI indices from June 2008 to May 2011. Positive/red (negative/blue) transports mean downwelling (upwelling) episode.

Much higher kinetic energy of circulation in Flores Sea was found during 'normal' year, weakened during El Nino year, and increased during La Nina year with one-month delay phase of inflow peaks. Seawater temperature within Ekman layer during the SEM period in El Nino 2009/2010 was anomalously much warmer than that during 'normal' year 2008. However, the thickness of Ekman layer in 'normal' year was much lower than that in El Nino year, and the shallowest Ekman layer occurred during La Nina year 2010/2011. The maximum divergent (negative) transport water mass that generates upwelling was revealed during 'normal' year, but minimum during La Nina year, due to positive transport (or downwelling) was maximum during La Nina year with short time duration, compared to 'normal' year.

Acknowledgments

The INDES0 model outputs were provided by CLS France. The Authors would like to thank INDES0 project office Jakarta, BPOL Bali, CLS and MERCATOR-Ocean Toulouse France, particularly to Dr. M. Eko Rudianto, Dr. Philippe Gaspar and Dr. Benoit Tranchant of CLS Toulouse. This study was partly financed by *KEMENRISTEK DIKTI* research grants 2016. Comments and suggestions from the Reviewers to improve this manuscript are highly appreciated.

References

- [1] Ilahude A G and Nontji A 1993 Oseanografi Indonesia dan Perubahan Iklim Global (El Nina dan La Nina). *Lokakarya Kita dan Perubahan Iklim Global: kasus El Nino-La Nina*. Akademi Ilmu Pengetahuan. Jakarta. 18-19 Mei.
- [2] Wyrtki K 1961 The physical oceanography of South East Asian Waters *Naga Report 2* (California: University California Press) 195p.
- [3] Gordon A L and Susanto R D 2001 Banda Sea surface-layer divergence *Ocean Dyn.* **52** 2-10. Doi: 10.1007/s10236-001-8172-6.
- [4] Ekman V W 1905 On the influence of the earth's rotation on ocean currents. *Arkiv. For Matematik, Astronomi och Fysik*, **2** 52

- [5] Madec G and Nemo Team 2008. *NEMO Ocean Engine*.
- [6] Tranchant B, Reffray G, Greiner E, Nugroho D, Koch-Larrouy A and Gaspar P 2015 Evaluation of an operational ocean modal configuration at 1/12° spatial resolution for the Indonesian seas - Part 1 *Oce Phys Geosci Model Dev. Disc.* **8** 6611-6668
- [7] Emery W J and Thomson R E 2004 *Data Analysis Methods in Physical Oceanography second and Revised Edition*. (Boulder: Colorado (USA))
- [8] Bingham F and Lukas R 1994 The Southward Intrusion of North Pacific Intermediate Water along the Mindanao Coast *J Phys Oceanogr.* **24** 141-154.
- [9] Gordon A L and Fine R A 1996 Pathways of water between the Pacific and Indian oceans in the Indonesian seas. *Nature.* **379** 146–149. doi:10.1038/379146a0.
- [10] Ilahude A G and Gordon A L 1996 Thermocline stratification within the Indonesian Seas. *J. Geophys. Res.* 101 12401-12409. doi: 10.1029/95JC03798.
- [11] Sprintall J, Gordon A L, Koch-Larrouy A, Lee T, Potemra J T, Pujiana K and Wijffels S E 2014 The Indonesian seas and their role in the coupled ocean-climate system *Nature Geoscience.* **7** 487-492. doi:10.1038/NNGEO2188.
- [12] Chang C P, Harr P A and Chen H J 2005 Synoptic disturbances over the equatorial South China Sea and western Maritime Continent during boreal winter *Monthly Weather Review* **133** 489-503.
- [13] Gordon A L, Susanto R D and Vranes K 2003 Cool Indonesian throughflow as a consequence of restricted surface layer flow *Nature.* **425** 824–828. doi:10.1038/nature02038.
- [14] Waworuntu J M, Fine R A, Olson D B and Gordon A L 2000 Recipe for Banda Sea water *J Mar Res.* **58** 547-569.
- [15] Zijlstr J J, Baars M A, Tijssen S B, Wetsteyn F J, Witte J I J, Ilahude A G and Hadikusumah 1990 Monsoonal effects on the hydrography of the upper waters (300 m) of the eastern Banda Sea and northern Arafura Sea, with special reference to vertical transport processes. *Neth. J. Sea Res.* **25** 431–447.
- [16] Cane M A and Zebiak S E 1985 A theory for El Nino and the southern oscillation *Science*.
- [17] Bradley R S and Lan W 2001 *Climate change and society* (Cheltenham Stanley: Thornes)
- [18] Horhoruw S M 2016 Struktur dan Variabilitas Arlindo di Selat Makassar [Tesis]. (Bogor (ID): Institut Pertanian Bogor)
- [19] Atmadipoera A S, Horhoruw S M, Purba M and Nugroho D Y 2016 Variasi spasial dan temporal Arlindo di Selat Makassar *ITKT.* **8** 299-320
- [20] Ffield A, Vranes K, Gordon A L and Susanto RD 2000 Temperature variability within Makassar Strait *J Geophys Res Lett.* **27** 237-240
- [21] Kadmaer E M Y 2013 Variabilitas klorofil-a dan beberapa parameter oseanografi, serta hubungannya dengan Monsoon, ENSO dan IOD di Laut Banda [Tesis]. (Bogor (ID): Institut Pertanian Bogor)
- [22] Moore T S, Marra J and Alkatiri A 2003 Response of the Banda Sea to the southeast monsoon *Mar. Ecol. Prog. Ser.* **261** 41-49
- [23] Atmadipoera A, Molcard R, Madec G, Wijffels, Sprintal J, Larrouy A K, Jaya I and Supangat A 2009 Characteristics and Variability of the Indonesian Throughflow Water at the Outflow Straits. *Deep Sea Research I.* **56** 1942-1954